In Vitro Analysis of Transport and Metabolism of 4'-Thiothymidine in Human Tumor Cells

David A. Plotnik[1], **Stephen Wu**[1], **Geoffrey R. Linn**[1], **Franco Chi Tat Yip**[1], **Natacha Lou Comandante**[1], **Kenneth A Krohn**[1,2], **Jun Toyohara**[3], and **Jeffrey L. Schwartz**[1,4]

[1]Department of Radiation Oncology, University of Washington, Seattle, WA USA

[2]Department of Radiology, University of Washington, Seattle, WA USA

[3]Research Team for Neuroimaging, Tokyo Metropolitan Institute of Gerontology, Tokyo, Japan

Abstract

Introduction—The use of thymidine (TdR) and thymidine analogs such as 3′-fluoro-3′-deoxythymidine (FLT) as positron emission tomography (PET)-based proliferation markers can provide information on tumor response to treatment. Studies on another TdR analog, 4'-thiothymidine (4DST), suggest that it might be a better PET-based proliferation tracer than either TdR or FLT. 4DST is resistant to the catabolism that complicates analysis of TdR in PET studies, but unlike FLT, 4DST is incorporated into DNA.

Methods—To further evaluate 4DST, the kinetics of 4DST transport and metabolism were determined and compared to FLT and TdR. Transport and metabolism of FLT, TdR and 4DST were examined in the human adenocarcinoma cell line A549 under exponential-growth conditions. Single cell suspensions were incubated in buffer supplemented with radiolabeled tracer in the presence or absence of nitrobenzylmercaptopurine ribonucleoside (NBMPR), an inhibitor of equilibrative nucleoside transporters (ENT). Kinetics of tracer uptake was determined in whole cells and tracer metabolism measured by high performance liquid chromatography of cell lysates.

Results—TdR and 4DST were qualitatively similar in terms of ENT-dependent transport, shapes of uptake curves, and relative levels of DNA incorporation. FLT did not incorporate into DNA, showed a significant temperature effect for uptake, and its transport had a significant NBMPR-resistant component. Overall 4DST metabolism was significantly slower than either TdR or FLT.

Conclusions—4DST provides a good alternative for TdR in PET and has advantages over FLT in proliferation measurement. However, slow 4DST metabolism and the short half-life of the ^{11}C label might limit widespread use in PET.

[4]Corresponding Author: Jeffrey L. Schwartz, Department of Radiation Oncology, Box 356069, University of Washington, Seattle, WA 98195 USA Phone: 12065984091, jschwart@uw.edu.

Keywords

PET Imaging; 4'-[methyl-^{11}C]thiothymidine; FLT; Nucleoside Metabolism

Introduction

One of the most relevant endpoints for evaluating tumor response to therapy is cell proliferation. Positron emission tomography (PET) provides a non-invasive approach to measure proliferation and response to therapy [1–3]. Thymidine (TdR) and thymidine analogs such as FLT (3′-fluoro-3′-deoxythymidine) and 4DST (4'-thiothymidine) have been used clinically as PET-based proliferation tracers [2, 4, 5]. Each has advantages and disadvantages. While TdR is efficiently incorporated into DNA, it is also rapidly catabolized by thymidine phosphorylase (TP), which complicates image analysis. TdR is a substrate for mitochondrial thymidine kinase 2 (TK2) as well as thymidine kinase 1 (TK1), this leads to TdR uptake in non-proliferating tissues with high mitochondria content like heart. Catabolism of TdR and TdR being a substrate for TK2, along with the short 20 minute half-life of ^{11}C used to label TdR, make the use of ^{11}C-TdR impractical for routine clinical PET measurements. By contrast, FLT is resistant to catabolism by TP, is a poor substrate for TK2, and can be labeled with ^{18}F, which has a longer half-life of 110 min. However, unlike TdR, FLT is not incorporated into DNA except as a chain terminator. Its ability to identify proliferating cells depends on its phosphorylation and retention by the growth-dependent enzyme TK1 [6, 7]. Like FLT, 4DST is resistant to catabolism by TP [4] and it shows low uptake in the heart wall [8], suggesting that it is a poor substrate for TK2. Like TdR, it is incorporated into DNA [4]. While it is limited by the short half-life of ^{11}C, Toyohara and colleagues suggest that the advantages of 4DST over both FLT and TdR outweigh the limitations associated with ^{11}C [4, 8, 9]. To further evaluate 4DST, we characterized the nature of its transport into cells as well as the kinetics of its metabolism.

Understanding nucleoside metabolism is important for qualifying interpretation of PET-based proliferation tracers. The kinetics of metabolism and knowledge of the rate-limiting steps in tracer metabolism help to validate the mechanism of uptake and loss of tracer signal *in vivo*. We measured the rates of 4DST metabolism, following each metabolite over a 2 h period, and compared these results to similarly measured rates of TdR and FLT metabolism.

While TK1 is an absolute requirement for FLT radiotracer accumulation [6, 10], variations in levels of the equilibrative nucleoside transporter-1 (ENT1) have been shown to modify intracellular peak levels of FLT [10–12]. We have reported that proliferating cells have higher levels of ENT1 than nonproliferating cells [10, 12]. Dependence of a proliferation tracer on ENT1 improves the ability of these tracers to distinguish between proliferating and nonproliferating regions of a tumor. In addition, higher ENT1 levels correspond to greater sensitivity to certain nucleoside-based chemotherapies [13–16], suggesting that FLT-PET imaging might be used to distinguish chemotherapy-sensitive tumors from resistant tumors [14, 17, 18]. For these reasons, in the present work we investigated the importance of ENT1 in the transport of 4DST.

MATERIALS AND METHODS

Materials

[methyl-^{3}H]-3′-Deoxy-3′-fluorothymidine ([^{3}H]-FLT; 351.5GBq/mmol), [methyl-^{3}H]-thymidine ([^{3}H]-TdR; 185 GBq/mmol), and [methyl-^{3}H]- 4'-thiothymidine ([^{3}H]-4DST; 233 GBq/mmol), were purchased from Moravek Biochemicals (Brea, CA). High-purity nitrobenzylmercaptopurine ribonucleoside (NBMPR) and other reagents were purchased from Sigma-Aldrich (St. Louis, MO). Cell culture media and supplements were purchased from Life Technologies (Carlsbad, CA).

Cell Culture Conditions

The human lung adenocarcinoma cell line A549 was used for all studies. Cell culture conditions were previously described [7]. Asynchronously cycling cells were maintained at sub-confluent levels. To measure both transport and metabolism, single cell suspensions were prepared by brief trypsin treatment and then incubated in tracer-containing buffers in water baths maintained at 20° or 37° C. Use of buffers simplified analysis by eliminating potential competition from TdR in the growth medium. Use of cell suspensions also allowed for more accurate determination of cell numbers and volume.

^{3}H-labeled Tracer Influx Studies

Tracer influx was carried out using single cell suspensions in sodium-containing 4-(2-hydroxyethyl)-1-piperazine ethanesulfonic acid (HEPES)-buffered Ringer's solution as described in [10, 19]. Parallel samples were supplemented with the human equilibrative nucleoside transporter (hENT) inhibitor NBMPR (10^{-4} M) to examine the role of equilibrative nucleoside transport [10, 19]. Tracer buffer concentrations ranged from 1–3×10^3 pmol/μL. Cold phosphate-buffered saline was added to stop influx at the desired time points, then cells were immediately pelleted and tracer-containing buffer rapidly aspirated. Cells were washed twice in excess cold phosphate buffered saline. Cell pellets were incubated overnight in 5% Triton X-100 at room temperature and radioactivity was measured in a Tri-Carb 1900 Liquid Scintillation Counter using Ultima Gold scintillation cocktail (Perkin Elmer). Cell numbers and average cell volume were determined from Coulter (Beckman Model Z2) measurements [6]. Experiments were performed in triplicate.

HPLC Analysis of Tracer Metabolites

For metabolism studies, cells were exposed to ^{3}H-labeled tracers and washed as described above, then put into cold 6% trichloroacetic acid (TCA). Samples were vortexed for 20 s, incubated on ice for 10 min, vortexed again, and centrifuged at 14,000×g for 10 min. The resulting supernatants were neutralized with saturated potassium bicarbonate and samples were analyzed using a Hewlett-Packard HP1050 high performance liquid chromatography (HPLC) system equipped with an in-line degasser (Alltech) and a Radiomatic 625TR flow scintillation analyzer (Perkin Elmer). A Waters Symmetry C$_{18}$ 3.5 μm (150×4.6mm) column equipped with a NovaPak C$_{18}$ guard column was used, and maintained at 27°C for all assays. HPLC details are found in [10]. A standard mixture containing TdR, thymidine monophosphate (TMP), FLT, and 4DST was run prior to each assay to validate metabolite

retention times. The flow scintillation analyzer was equipped with a 1000μL flow cell, and Ultima-Flo AP (Perkin Elmer) liquid scintillation cocktail was delivered at a rate of 3.0 mL/min. HP Chemstation software (Hewlett Packard) was used to pilot the HPLC and ProFSA Plus software (Perkin Elmer) was used to plot the flow scintillation analyser output and for data analysis. The counting efficiency of the detector under these conditions was 60.3%. In parallel reactions, radioactivity in the acid precipitate and supernate samples was measured in a Tri-Carb 1900 Liquid Scintillation Counter using Ultima Gold scintillation cocktail (Perkin Elmer). These values were used to ensure all intracellular radioactivity was accounted for in the metabolite analysis, and radioactivity in the precipitate served as a measure of DNA tracer incorporation. Assays were performed in triplicate.

RESULTS

Tracer Transport and Uptake

Thymidine—TdR tracer uptake over a 120 minute period generally fit a hyperbolic parabolic curve, with rapid uptake from 0–30 min followed by slower uptake from 30–120 min (Figure 1A). Uptake curves measured at 20° C or 37° C had similar shapes and similar initial rates of uptake, but appeared to differ slightly in final rates. Total intracellular TdR activity was $1.18 \pm 0.51 \times 10^5$ pmol/10^6 cells after 120 min incubation at 37°C and $9.84 \pm 0.99 \times 10^4$ pmol/10^6 cells after 120 min at 20° C.

To assess the degree of tracer accumulation, intracellular TdR activity was plotted as a percentage of TdR activity in the uptake buffer. The curves for TdR concentration (Figure 1D) were similar in shape to total cell activity. Intracellular TdR concentration was 60-fold greater than buffer levels after 120 min incubation at 37° C and 51-fold greater after 120 min incubation at 20° C. As expected, these values were much greater than previously reported values for cultures of non-cycling A549 cells [10].

Nucleoside transporters, particularly ENT1 [20, 21], are important for transport of TdR into cells [10, 11, 17, 19]. ENT-dependent uptake was assessed by performing experiments in the presence of saturating concentrations of the ENT inhibitor NBMPR. NBMPR reduced TdR uptake by $98.1 \pm 0.9\%$ (Figure 1A). NBMPR-resistant transport was very slow and resulted in a modest 2-fold higher intracellular concentration of TdR above buffer levels at 120 min for 20° C incubations and at 60 min for 37° C incubations (Figure 1D). The curves for NBMPR-resistant TdR concentration (Figure 1D) were similar in shape to that observed for total cell activity (Figure 1A).

3′-Fluoro-3′-deoxythymidine—FLT uptake measured at 37° C over a 120 minute period generally fit a curve where uptake reached a maximum at 60 min, then decreased slightly for the remaining 60 min of incubation (Figure 1B). Unlike TdR, the kinetics of FLT uptake during incubation at 37° C was very different from kinetics of uptake at 20° C. Uptake at 20° C was linear over the 120 min incubation. The initial rate of FLT uptake appeared greater at 37° C than at 20° C, but the total intracellular FLT after 120 min at 37° C was consistently half of that for cells incubated at 20° C ($3.27 \pm 0.17 \times 10^4$ pmol/10^6 cells). In a previous publication [22], we reported evidence for a deoxynucleotidase that degraded FLT-MP to FLT in A549 cells incubated at 37° C and led to FLT loss from cells. This could

account for the apparent plateau in FLT uptake in figure 1B. The absence of this effect in cells incubated at 20° C suggests energy dependency for either the nucleotidase or the downstream nucleotide diphosphate kinase.

The curves for intracellular concentration normalized to buffer activity (Figure 1E) were similar in shape to the FLT activity curves (Figure 1B). There was a 16.4-fold increase of intracellular FLT over buffer levels after 120 min incubation at 37° C and a 33.2-fold increase after 120 min incubation at 20° C. The corresponding values for 15min incubations were an 11.7-fold increase at 37° C and a 7.7-fold increase after incubation at 20° C.

NBMPR reduced FLT uptake by $64.1 \pm 14.2\%$ (Figure 1B, 1E). As previously reported [10], NBMPR slowed concentration of tracer but did not completely block it as with TdR (Figure 1A, 1C). The effect of NBMPR on the slopes of uptake was similar for incubation at both 37° C and 20° C, which might reflect NBMPR also blocking FLT efflux.

4'-Thiothymidine—4DST tracer uptake over a 120 min period was biphasic with rapid uptake from 0–30 min followed by slower uptake from 30–120 min (Figure 1C). Unlike TdR, the uptake curve was not hyperbolic and did not reach a plateau. The kinetics of 4DST uptake at both 20° C and 37° C were similar in shape (Figure 1C), but like TdR, slightly higher rates of uptake were observed in cells incubated at 37° C ($1.23 \pm 0.18 \times 10^4$ pmol/10^6 cells after 120 min) as compared to 20° C ($1.08 \pm 0.03 \times 10^4$ pmol/10^6 cells after 120 min). Uptake of 4DST was approximately $1/10^{th}$ the uptake of TdR.

While the initial rate of FLT uptake at 37° C was about 3-fold greater than the corresponding value for 4DST, the total cell activity after a 120 min incubation at 37° C ($1.61 \pm 0.05 \times 10^4$ pmol/10^6 cells) was only slightly greater than that seen for 4DST. The time course for 4DST (Figure 1C) suggests one could potentially see higher levels of 4DST uptake as compared to FLT when incubation times substantially longer than the half-life of ^{11}C are used. This would be in agreement with previously published work [9] that reported higher levels of 4DST uptake as compared to FLT.

4DST was concentrated 12.5-fold compared to buffer in cells incubated for 120 min at 37° C and approximately 7.5-fold in cells incubated at 20° C (Figure 1E). These values represent 15 – 20% of the TdR values.

NBMPR reduced 4DST uptake by $82.5 \pm 4.0\%$ (Figure 1C). This value does not reflect a greater NBMPR-resistant component of 4DST uptake compared to TdR, since both nucleosides accumulated to similar levels in the presence of NBMPR. Instead, this value indirectly reflects the relatively low levels of 4DST uptake compared to TdR. NBMPR effectively prevented tracer concentration over buffer levels (Figure 1F). As with TdR, NBMPR-resistant uptake was slow, and slightly greater with incubation at 37°C versus 20°C. For cells incubated at 20° C, intracellular concentrations of activity reached equilibrium with buffer after 30min and remained at this level for the remaining 90min (Figure 1F). For cells incubated at 37° C, equilibrium was observed at 15min and there was evidence of some small concentration above buffer levels beyond this time.

Nucleoside Metabolism

Metabolites of each of the three nucleosides were measured in asynchronous cultures of A549 cells incubated at 20° C in tracer-containing buffer. Incubation at 20° C was used to avoid the loss of FLT from cells incubated for 60 – 120 min at 37° C. We have previously reported on FLT metabolism at 37° C [22]. Nearly 100% of the total intracellular radioactivity was accounted for in the metabolite analysis for all three tracers, but the three tracers had very different metabolism kinetics.

TdR was rapidly metabolized to thymidine triphosphate (TdR-TP) and reached a plateau around $5{\times}10^4$ pmol/10^6 cells by 60 min (Figure 2A). Activity in DNA (acid-precipitate fraction) increased linearly with time reaching $3.7{\times}10^4$ pmol/10^6 cell-equivalents by 120 min. Levels of TdR and TdR metabolites were relatively low over the entire time course. The results are consistent with a rapid rate of TdR phosphorylation to TdR-TP and reaction with DNA polymerase.

In contrast to TdR, intracellular FLT was predominately present as FLT-monophosphate (FLT-MP) (Figure 2B). Levels of FLT-MP increased up to about $1.5{\times}10^4$ pmol/10^6 cells by 120 min. FLT-triphosphate (FLT-TP) began accumulating at 30 min and its levels increased linearly, reaching $1.6{\times}10^4$ pmol/10^6 cells by 120 min. As with TdR, levels of FLT and FLT diphosphate were relatively low over the entire time course. As was expected, FLT was not observed to incorporate into DNA.

The kinetics of metabolism of 4DST was much slower and more complex than that seen with either TdR or FLT (Figure 2C). Levels of the nucleoside peaked at 30min and then declined. 4DST monophosphate (4DST-MP) levels peaked at 30 min and then remained at this level for the remaining 90 min incubation time. 4DST-triphosphate (4DST-TP) levels peaked at $2.5{\times}10^3$ pmol/10^6 cells at 60 min before declining to about 500 pmol/10^6 cells at 120 min. There was an apparent exponential increase in activity in DNA reaching $6.0{\times}10^3$ pmol/10^6 cells by 120 min. By 120 min, label in DNA made up most of the intracellular activity.

DISCUSSION

Our results suggest the transport of 4DST is qualitatively similar to that of TdR. Under our experimental conditions, both tracers were transported almost entirely by NBMPR-sensitive transporters. Both were minimally affected by reducing temperature from 37° C to 20° C, and for both, a significant proportion of the intracellular activity observed after 120 minutes was associated with DNA. However, there were significant quantitative differences between the tracers: overall intracellular activity after a 2 hour uptake period was 10-fold higher for TdR than 4DST. These findings may be explained by differences in the metabolism of TdR and 4DST. For both TdR and 4DST, intracellular nucleoside, monophosphate metabolite, and diphosphate metabolite were present in similar quantities and were stable for the 120min incubation period. By contrast, TdR-TP accumulated rapidly and stabilized at high levels, while 4DST-TP accumulated slowly and appeared to be depleted between 60 and 120min. This depletion of 4DST-TP coincided with increased incorporation of 4DST into DNA.

These observations suggest the conversion of 4DST-DP to 4DST-TP may be slow, or that 4DST-TP may be less stable than TdR-TP.

In contrast to both TdR and 4DST, FLT transport was only partially inhibited by NBMPR. There was also a significant temperature effect for FLT uptake, as intracellular activity after a 2 hour uptake period was much higher at 20°C compared to 37°C. We hypothesize that this may be due to loss of FLT from the cell via a deoxynucleotidase that is active at 37°C but not at 20°C. Finally, as expected there was no concentration of FLT activity in DNA. Despite this difference, intracellular levels of FLT and 4DST were nearly equivalent after a 2 hour incubation at 37°C, potentially because of loss of FLT from the cell. Therefore, as suggested by Toyohara and colleagues [4, 8, 9, 23], 4DST has advantages over FLT in that it better mimics TdR and can be incorporated into DNA. This would provide a more robust measure of DNA synthesis. While *in vivo* imaging studies demonstrate potential for 4DST in PET imaging [8, 24, 25], the longer scanning times needed for 4DST might limit its usefulness because of the relatively short half-life of the ^{11}C label.

Conclusions

4DST provides a good alternative for TdR in PET analysis because it is a TK1-specific substrate and is resistant to catabolism by thymidine phosphorylase (TP). It also provides a potentially better marker of proliferation as compared to FLT because its transport is mediated strongly by ENT1 and its activity is incorporated into DNA: there is no retrograde loss of signal. Slow 4DST metabolism will limit routine use in PET because of the short half-life of the ^{11}C label.

ACKNOWLEDGEMENT

REFERENCES

1. Krohn KA, Mankoff DA, Eary JF. Imaging cellular proliferation as a measure of response to therapy. J Clin Pharmacol. 2001; (Suppl):96S–103S. [PubMed: 11452736]

2. Krohn KA. Evaluation of alternative approaches for imaging cellular growth. Q J Nucl Med. 2001; 45:174–178. [PubMed: 11476167]

3. Spence AM, Muzi M, Krohn KA. Molecular imaging of regional brain tumor biology. J Cell Biochem Suppl. 2002; 39:25–35. [PubMed: 12552599]

4. Toyohara J, Kumata K, Fukushi K, Irie T, Suzuki K. Evaluation of 4'-[methyl-14C]thiothymidine for in vivo DNA synthesis imaging. J Nucl Med. 2006; 47:1717–1722. [PubMed: 17015909]

5. Shields AF. PET imaging with 18F-FLT and thymidine analogs: promise and pitfalls. J Nucl Med. 2003; 44:1432–1434. [PubMed: 12960188]

6. Rasey JS, Grierson JR, Wiens LW, Kolb PD, Schwartz JL. Validation of FLT uptake as a measure of thymidine kinase-1 activity in A549 carcinoma cells. J Nucl Med. 2002; 43:1210–1217. [PubMed: 12215561]

7. Schwartz JL, Tamura Y, Jordan R, Grierson JR, Krohn KA. Monitoring tumor cell proliferation by targeting DNA synthetic processes with thymidine and thymidine analogs. J Nucl Med. 2003; 44:2027–2032. [PubMed: 14660729]

8. Toyohara J, Nariai T, Sakata M, Oda K, Ishii K, Kawabe T, et al. Whole-body distribution and brain tumor imaging with (11)C-4DST: a pilot study. J Nucl Med. 2011; 52:1322–1328. [PubMed: 21764794]

9. Toyohara J, Okada M, Toramatsu C, Suzuki K, Irie T. Feasibility studies of 4'-[methyl-(11)C]thiothymidine as a tumor proliferation imaging agent in mice. Nucl Med Biol. 2008; 35:67–74. [PubMed: 18158945]

10. Plotnik DA, Emerick LE, Krohn KA, Unadkat JD, Schwartz JL. Different modes of transport for 3H-thymidine, 3H-FLT, and 3H-FMAU in proliferating and nonproliferating human tumor cells. J Nucl Med. 2010; 51:1464–1471. [PubMed: 20720049]

11. Paproski RJ, Ng AM, Yao SY, Graham K, Young JD, Cass CE. The role of human nucleoside transporters in uptake of 3'-deoxy-3'-fluorothymidine. Mol Pharmacol. 2008; 74:1372–1380. [PubMed: 18669604]

12. Plotnik DA, Asher C, Chu SK, Miyaoka RS, Garwin GG, Johnson BW, et al. Levels of human equilibrative nucleoside transporter-1 are higher in proliferating regions of A549 tumor cells grown as tumor xenografts in vivo. Nucl Med Biol. 2012; 39:1161–1166. [PubMed: 22985987]

13. Hubeek I, Stam RW, Peters GJ, Broekhuizen R, Meijerink JP, van Wering ER, et al. The human equilibrative nucleoside transporter 1 mediates in vitro cytarabine sensitivity in childhood acute myeloid leukaemia. Br J Cancer. 2005; 93:1388–1394. [PubMed: 16333246]

14. Paproski RJ, Young JD, Cass CE. Predicting gemcitabine transport and toxicity in human pancreatic cancer cell lines with the positron emission tomography tracer 3'-deoxy-3'-fluorothymidine. Biochem Pharmacol. 2009; 79:587–595. [PubMed: 19788890]

15. Santini D, Vincenzi B, Fratto ME, Perrone G, Lai R, Catalano V, et al. Prognostic role of human equilibrative transporter 1 (hENT1) in patients with resected gastric cancer. J Cell Physiol. 2010; 223:384–388. [PubMed: 20082300]

16. Tsujie M, Nakamori S, Nakahira S, Takahashi Y, Hayashi N, Okami J, et al. Human equilibrative nucleoside transporter 1, as a predictor of 5-fluorouracil resistance in human pancreatic cancer. Anticancer Res. 2007; 27:2241–2249. [PubMed: 17695509]

17. Perumal M, Pillai RG, Barthel H, Leyton J, Latigo JR, Forster M, et al. Redistribution of nucleoside transporters to the cell membrane provides a novel approach for imaging thymidylate synthase inhibition by positron emission tomography. Cancer Res. 2006; 66:8558–8564. [PubMed: 16951168]

18. Kenny LM, Contractor KB, Stebbing J, Al-Nahhas A, Palmieri C, Shousha S, et al. Altered tissue 3'-deoxy-3'-[18F]fluorothymidine pharmacokinetics in human breast cancer following capecitabine treatment detected by positron emission tomography. Clin Cancer Res. 2009; 15:6649–6657. [PubMed: 19861447]

19. Plotnik DA, McLaughlin LJ, Chan J, Redmayne-Titley JN, Schwartz JL. The role of nucleoside/nucleotide transport and metabolism in the uptake and retention of 3'-fluoro-3'-deoxythymidine in human B-lymphoblast cells. Nucl Med Biol. 2011; 38:979–986. [PubMed: 21982569]

20. Ward JL, Sherali A, Mo ZP, Tse CM. Kinetic and pharmacological properties of cloned human equilibrative nucleoside transporters, ENT1 and ENT2, stably expressed in nucleoside transporter-deficient PK15 cells. Ent2 exhibits a low affinity for guanosine and cytidine but a high affinity for inosine. J Biol Chem. 2000; 275:8375–8381. [PubMed: 10722669]

21. Szkotak AJ, Ng AM, Sawicka J, Baldwin SA, Man SF, Cass CE, et al. Regulation of K(+) current in human airway epithelial cells by exogenous and autocrine adenosine. Am J Physiol Cell Physiol. 2001; 281:C1991–C2002. [PubMed: 11698258]

22. Grierson JR, Schwartz JL, Muzi M, Jordan R, Krohn KA. Metabolism of 3'-deoxy-3'-[F-18]fluorothymidine in proliferating A549 cells: validations for positron emission tomography. Nucl Med Biol. 2004; 31:829–837. [PubMed: 15464384]

23. Toyohara J, Sakata M, Oda K, Ishii K, Ishiwata K. Longitudinal observation of [11C]4DST uptake in turpentine-induced inflammatory tissue. Nucl Med Biol. 2013; 40:240–244. [PubMed: 23141551]

24. Minamimoto R, Toyohara J, Ito H, Seike A, Miyata Y, Morooka M, et al. A pilot study of 4'-[methyl-11C]-thiothymidine PET/CT for detection of regional lymph node metastasis in non-small cell lung cancer. EJNMMI Res. 2014; 4:10. [PubMed: 24593883]

25. Minamimoto R, Toyohara J, Seike A, Ito H, Endo H, Morooka M, et al. 4'-[Methyl-11C]-thiothymidine PET/CT for proliferation imaging in non-small cell lung cancer. J Nucl Med. 2012; 53:199–206. [PubMed: 22190643]
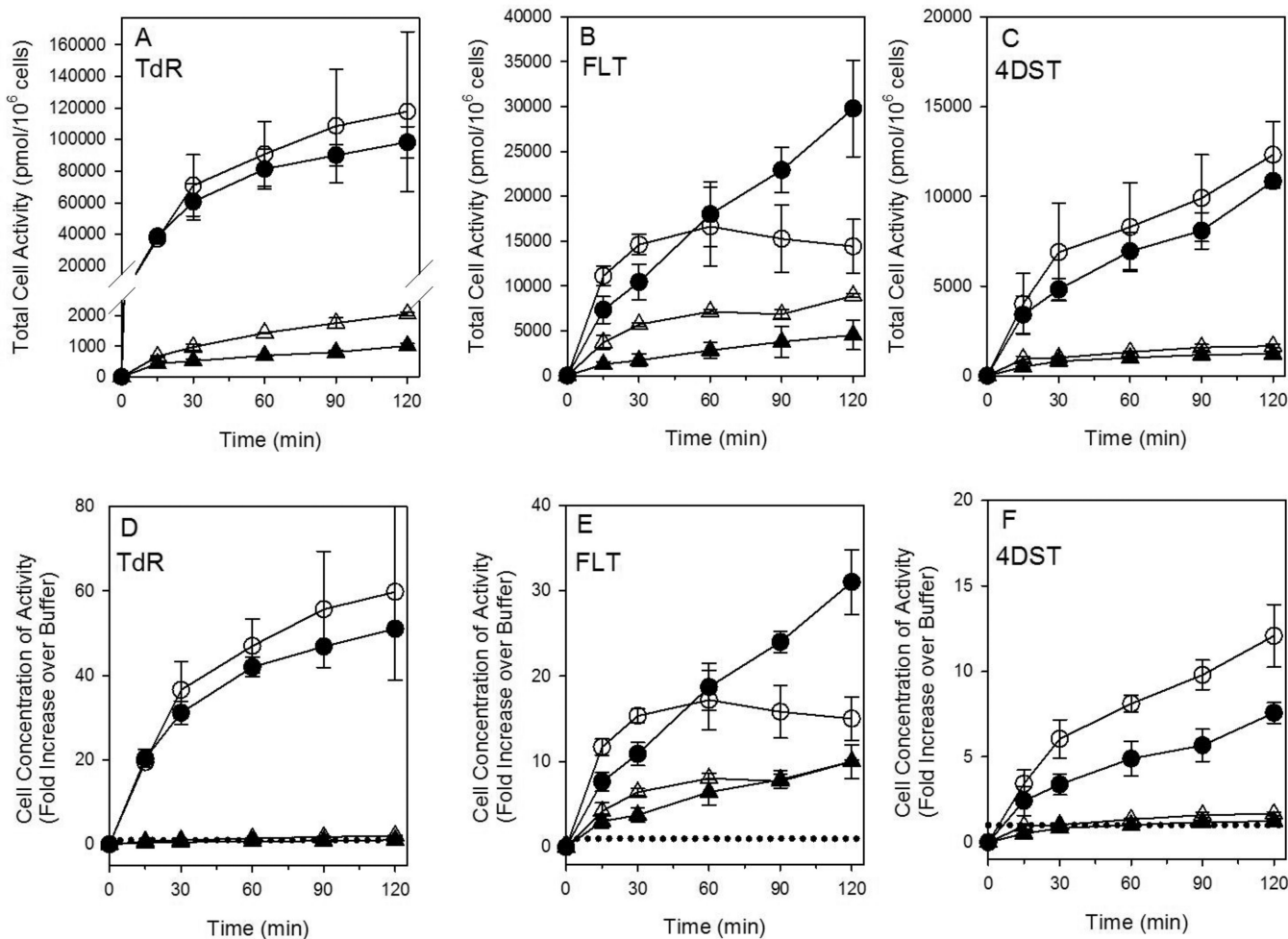
Figure 1.

Time-Dependent Nucleoside Uptake in A549 Cells. (A, B, C) Intracellular levels of tracer (pmol/10^6 cells) in asynchronous single cell suspensions incubated in tracer-containing buffer at 37° C (open symbols) or 20° C (filled symbols). (D, E, F) Fold increase in intracellular levels of tracer (activity in cells normalized to activity in an equivalent volume of buffer set to 1) in asynchronous cells incubated in tracer-containing buffer at 37° C (open symbols) or 20° C (filled symbols). Panel A, D: TdR, Panel B, E: FLT, Panel C, F: 4DST. Tracer containing buffer alone: (○, ●). Tracer containing buffer supplemented with 10^{-4}M NBMPR (, ▲). Dotted Line: Activity representing equal levels of activity in cells and buffer.
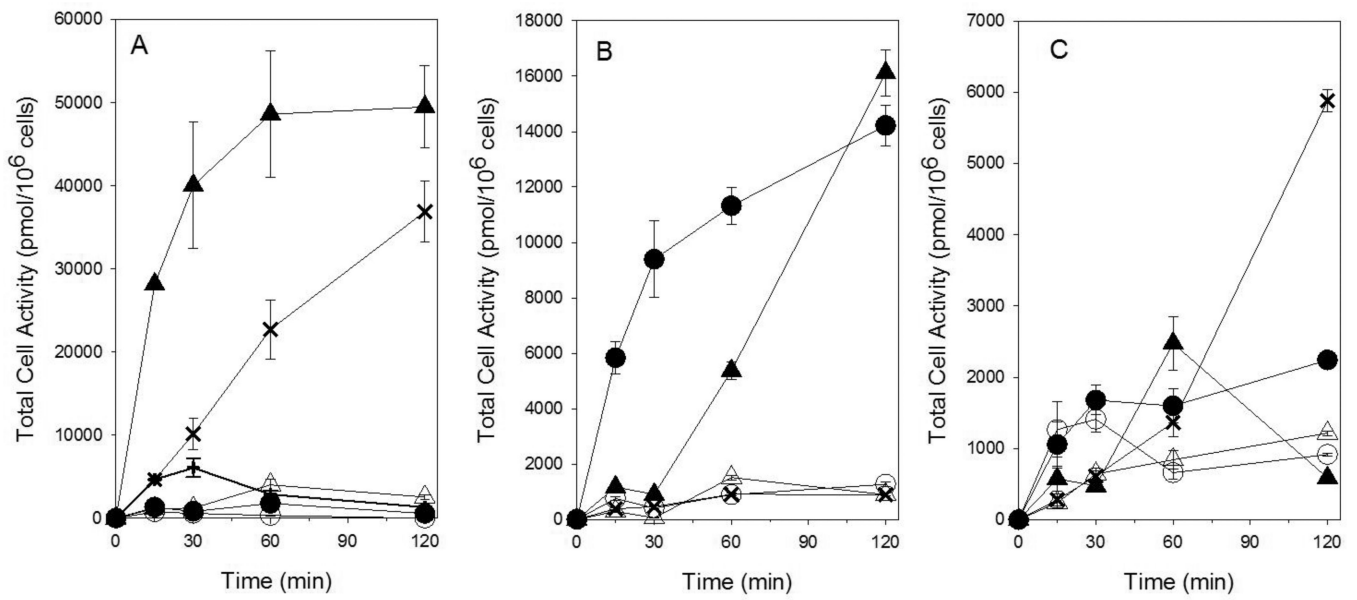
Figure 2.
Time-Dependent Tracer Metabolism in A549 Cells Assayed as Asynchronous, Exponential
Cultures Incubated at 20° C in Buffer Containing (A) TdR, (B) FLT, or (C) 4DST.
Nucleoside (○), Monophosphate (●), Diphosphate ( ), Triphosphate (▲), DNA (X) and
Thymine (+).